Analytical Seismic Fragility Curves for Reinforced Concrete Wall pier using Shape Memory Alloys considering maximum drift

Nursafarina Ahmad[1,2,*], *Azmi* Ibrahim[1], and *Shahria* Alam[2],

[1]Faculty of Civil Engineering, Universiti Teknologi MARA, Shah Alam, 40450 Selangor, Malaysia
[2]School of Engineering, University of British Columbia, V1V1V7 Kelowna, British Columbia, Canada

Abstract. Fragility curves express the seismic vulnerability of bridge piers for different damage states at various earthquake intensities. A fragility curve typically gives a physical understanding of repair costs and functionally levels of a bridge pier. Shape memory alloys (SMAs) provide a promising alternative material in reducing the failure probability of a bridge pier. This study develops a family of seismic fragility curves for reinforced concrete (RC) wall piers reinforced with three different types of SMA rebar in plastic hinge regions. An incremental dynamic analysis (IDA) using a total of 20 earthquake ground motions was performed on a SMA-RC wall pier to evaluate its seismic performance. The maximum drift recorded for each ground motion was taken as the seismic performance demand parameter of interest in this study. The probabilistic seismic demand model (PSDM) was used to generate fragility curves for each RC-SMA wall pier. The results show that the different mechanical properties and type of SMAs affect the performance of RC-SMA wall pier.

1 Introduction

Performance-based seismic design of bridges is now more frequently reviewed as it is necessary to enhance the ductility and limit the residual deformation of bridge structures due to the widespread damage of structures caused by earthquakes activities. Current seismic design codes such as EC8-2 [1], JRA 2012 [2], CHBDC 2014 and AASHTO LRFD 2012 [3-4] have provisions for performance based seismic design that allows reinforced concrete (RC) bridges to be designed with the ability to dissipate energy without causing any residual deformation during a seismic event. However, past catastrophic earthquakes events such as the Loma Prieta earthquake in 1989, the Northridge earthquake in 1994 and the Kobe earthquake in 1995 demonstrated that RC bridges were still vulnerable to seismic loading with most affected structures suffered serious damage and some even collapsed.

The overall seismic response of a bridge is dependent on the response of its pier. Evidence from the 1989 Loma Prieta earthquake shows collapse of Cypress Street Viaduct bridge while field reports reveal bridge piers suffering most from the strong earthquake ground motions. Considering the importance of bridges in maintaining the post-earthquake functionality of bridges [5], it is necessary to evaluate the seismic vulnerability of bridges. Fragility curves provide an important decision making tool in assessing the seismic risk of structures being damaged by different ground motion levels. In principle, there are different methodologies and approaches that have been developed for evaluating the seismic fragility of bridges [5]. The methodologies for the development of fragility curves include expert judgments [6], empirical approaches [7-8], and experimental and analytical approaches [9-12].

Over the last few years, many researchers [13-15] have found the ability of shape memory alloys (SMAs) as one of the rival materials for reinforcement bars in RC structures and their findings are well-documented. SMAs belong to a class of shape memory materials which have many advantages including large resistance to corrosion and high recoverable residual deformation. Many studies concluded that SMAs have significant positive effects on mitigating deficiencies of seismic resistance of conventional bridges and enhancing the performance of bridges under earthquake ground motions [16-18].

Several studies attempted to investigate the seismic vulnerability of bridges reinforced with SMAs [19-21], expressing their seismic risks in the form of fragility curves. A recent study by Billah and Alam [22] has developed fragility curves representing the seismic risk of bridge piers reinforced with five different types of SMA. The results demonstrated that all SMA-reinforced bridge piers exhibited a low probability of collapse in terms of maximum drift, thus effectively reducing the overall seismic vulnerability of the bridge piers. In this paper, seismic fragility curves for concrete wall piers

* Corresponding author: nursafarinaahmad@gmail.com; nursafarina1131@salam.uitm.edu.my

reinforced with three different types of shape memory alloy considering maximum drift as the single demand parameter. The evaluation of the seismic fragility of the SMA-reinforced concrete (SMA-RC) wall piers is based on an analytical approach. A total of 20 selected earthquakes scaled with peak ground acceleration ranging from 0.101g to 0.875g was used in a nonlinear incremental dynamic analysis (IDA) [23] on each SMA-RC wall pier and the maximum drift recorded for each ground motion at each levels of intensity up to an intensity of 2.0g. The probabilistic seismic demand model (PSDM) is used to generate the fragility curves. Finally, seismic fragility curves for three different SMA-RC wall piers are compared.

2 Fragility function methodology

Fragility curves are a seismic risk tool that represents the vulnerability of a bridge influenced by a specified range of ground motion intensity in terms of probability distribution functions. The development of fragility curves can be used as an effective strategy to increase the level of safety of highway bridges, and to improve the decision making process for the estimation of loss and risk mitigation. Fragility function can be expressed as [24]

$$\text{Fragility} = P\,(LS \mid IM=y) \tag{1}$$

where P (LS | IM=y) is the probability of exceeding a damage state as a function of engineering demand parameters (EDPs) at a given ground motion with IM=y. The present study makes use of the PSDM to generate fragility curves from the IDA results. A power law function [25] was assumed to obtain the mean and standard deviation through a regression analysis for each limit state, which provides a logarithmic correlation between a median demand and a selected IM.

$$EDP = a\,(IM)^b \tag{2}$$

$$\ln(EDP) = \ln a + b \ln(IM) \tag{3}$$

where, a and b are unknown coefficients which can be estimated from a regression analysis of the response data collected from the IDA. The EDPs are assumed to follow a lognormal distribution. Equation 4 [26] is used to estimate the dispersion of the demand (βEDP| IM), conditioned upon the IM.

$$\beta_{EDP/IM} = \sqrt{\frac{\sum_{i=1}^{N}[ln(EDP_i) - ln(a(IM_i)^b]^2}{N-2}} \tag{4}$$

where, N is the number of simulations. It is now possible to generate the fragilities using Equation 5 [27] with the PSDM and the limit states corresponding to various damage levels.

$$P[LS/IM] = \varphi\frac{\ln(IM) - \ln(IM_n)}{\beta_{comp}} \tag{5}$$

where

$$\ln(IM_n) = \frac{\ln(Sc) - \ln(a)}{b} \tag{6}$$

$$\beta_{comp} = \sqrt{\frac{\beta_{EDP/IM} + \beta_c^2}{b}} \tag{7}$$

ln (IM_n) is defined as the median value of the intensity measure for the damage state (i.e slight, moderate, extensive, collapse), a and b are the regression coefficients and the dispersion component is given in Equation 7. [27] where, Sc is the median and βc is the dispersion value for each damage state.

3 Wall pier configuration

The wall piers are seismically designed and assumed to be located in Vancouver, British Columbia Canada (Fig.1). A 2% probability of exceedance in 50 years (2475 years) is selected for design spectrum according to the CHBDC-2014 [3].

Table 1. Properties of different types of SMA

Alloy	E (GPa)	f_y (MPa)	f_{p1} (MPa)	f_{t1} (MPa)	f_{t2} (MPa)	ε_s (%)
CuAlMn [1]	28	210	0.48	275	150	9
FeMnAlNi [2]	98.4	320	0.39	442.5	122	6.13
$NiTi_{45}$ [3]	68	435	0.49	535	170	8

E = modulus of elasticity; f_y= austenite to martensite starting stress; f_{p1}= Austenite to Martensite finishing stress; f_{t1}= Martensite to Austenite starting stress; f_{t2}= Martensite to Austenite finishing stress; and ε_s = superelastic plateau strain

SMA bars are used only at the bottom of the plastic hinge region of all the RC-SMA wall piers. The three types of SMA used in this study and their mechanical properties are shown in Table 1. The Paulay and Priestley equation [28] is used to calculate the length of a plastic hinge, Lp, for the concrete wall pier reinforced with SMA. The equation is:

$$L_p = 0.08L + 0.022\,d_b f_y \tag{8}$$

Here, Lp is the member length in mm; db is the reinforcement diameter in mm and fy is the yield strength of the bar in MPa.

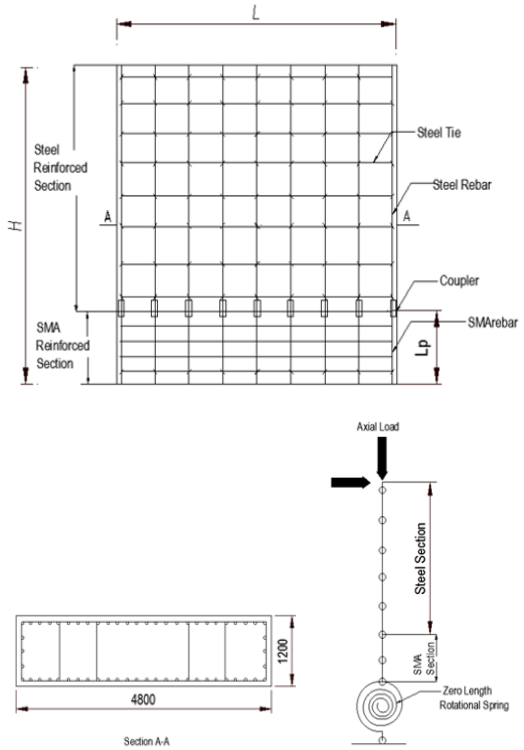

Fig. 1. (a) Elevation (b) cross section A-A (c) finite element model of RC-SMA wall pier

4 Finite Element Modeling

Seismostruct [29] was used to model the reinforced concrete wall piers reinforced with shape memory alloys. The SMA-RC wall piers were modelled using nonlinear beam-column elements with rectangular cross-sections. The uniaxial stress-strain concrete material constitutive law based on Mander et al. [30] was used to model both the unconfined and confined concrete in the appropriate regions of the SMA-RC wall pier cross-sections. The transverse and longitudinal steel reinforcements bars were modelled using the Menegotto Pinto model [31]. The Auricchio and Sacco model [32] was used to represent the SMA reinforcement using the parameters in Table 1. SMAs were only used as a vertical rebar at the bottom of the plastic hinge of the RC wall piers. In addition, a zero-length rotational spring element was introduced at the bottom of the column section (Fig. 1c) to represent the mechanical couplers used to connect the steel to the SMA reinforcements. A bond- slip model with modified Takeda hysteretic curve [33] was used to model the slippage of SMA reinforcement bar from the coupler following the work of Billah and Alam [13] who numerically validated the bond slip relation for a SMA rebar against the experimental study by Alam et al. [34].

5 Fragility assessment of SMA-RC wall pier

The fragility curves were developed based on the PSDM with the maximum drift taken as the engineering demand parameter. 20 different ground motions (Table 2) from the PEER strong motion database of different magnitudes and peak ground accelerations (PGAs) were selected for the IDA. SeismoMatch [34] was used to match all the 20 ground motion records to the Vancouver's target response spectrum with a 5% damping ratio as shown in Fig. 2.

Table 2. Characteristics of the earthquake records

No	Earthquake	Year	*M	Distance (km)	PGA (g)
1	Chi-Chi	1999	7.6	10.4	0.157
2	Friuli	1976	6.5	10.8	0.11
3	Imperial Valley	1979	6.5	28.7	0.27
4	Imperial Valley	1979	6.5	21.9	0.117
5	Imperial Valley	1979	6.5	28.7	0.254
6	Landers	1992	7.3	10.3	0.283
7	Loma Prieta	1989	6.9	12.7	0.367
8	Loma Prieta	1989	6.9	10.3	0.453
9	Loma Prieta	1989	6.9	3.5	0.46
10	Loma Prieta	1989	6.9	28.8	0.371
11	Morgan Hill	1984	6.2	28.3	0.101
12	Northridge	1994	6.7	22.6	0.514
13	Northridge	1994	6.7	22.2	0.252
14	Northridge	1994	6.7	7.5	0.87
15	Northridge	1994	6.7	6.4	0.72
16	San Fernando	1971	6.6	21.1	0.174
17	Superstition Hill	1987	6.7	24.4	0.134
18	Superstition Hill	1987	6.7	24.4	0.132
19	Kobe	1995	6.9	4.3	0.56
20	Kobe	1995	6.9	3.4	0.77

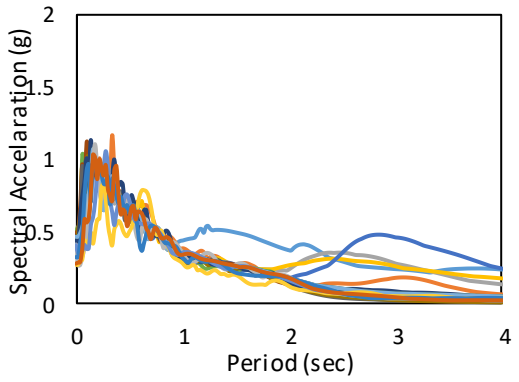

Fig. 2. Selected 20 earthquake ground motion records for spectral acceleration.

The maximum drifts (MDs) of the wall piers which represent the different performance-based limit states were considered as the EDP. An IDA was performed on the wall piers under a set of scaled intensity measures (IMs) with a constant increment of 0.2g up to 2.0g of the selected earthquake records using SeismoStruct [30]. The maximum drift of RC-SMAs wall pier subjected to 20 scaled earthquakes were recorded for each PGA level. The IMs are the first mode spectral accelerations, Sa (T1). In the present study, a PGA was considered an IM due to its practically, sufficiency and efficiency to analyse structural seismic fragilities [35-36].

Table 3. PSDMs for maximum drift

	Maximum drift		
Wall pier type	*a*	*b*	*β EDP| IM*
RC-SMA1	2.04	1.06	0.48
RC-SMA2	1.77	1.18	0.39
RC-SMA3	2.16	1.09	0.49

PSDMs are generated from the relationship between EDP and IM through a linear regression in a log-transformed space. Fig. 3 shows the PSDMs for the three different RC-SMA wall piers considering the maximum drift as the EDP. The slope, intercept and dispersion of the EDP|IM relationship were carried out from this linear regression model and shown in Table 4. A strong relationship between EDP and IM is evident from Fig.3 with R2 values higher than 0.8 for all the PSDMs. Table 3 summarizes the demand dispersion (βEDP| IM) for all the RC-SMA wall piers where RC-SMA1 wall pier yielded a higher dispersion in demand than the RC-SMA2, and both the RC-SMA1 and RC-SMA3 wall piers have almost a similar dispersion in demand (βEDP| IM) indicating the effectiveness of introducing the right SMAs in the right regions in reducing maximum drifts of a wall pier.

Table 4. Limit state capacity of RC-SMA wall pier.

Damage State		Maximum drift					
		RC-SMA1		RC-SMA2		RC-SMA3	
		Sc	β_c	Sc	β_c	Sc	β_c
DS-1	Cracking	0.21	0.21	0.21	0.21	0.21	0.21
DS-2	Yielding	1.72	0.27	1.26	0.27	1.68	0.27
DS-3	Spalling	1.35	0.41	1.32	0.41	1.33	0.41
DS-4	Crushing	3.94	0.44	3.59	0.44	3.83	0.44

Four damage levels namely slight, moderate, extensive and collapse were considered in accordance with HAZUS [37]. The damage states are quantified based on the performance limit states proposed by Hose et al [39]. The performance limit states considered here are the drift percentages for cracking of concrete, yielding of reinforcements, and spalling and crushing concrete, and they are based on a strain damage approach. Yielding of SMA rebar was defined by the yield strain of the SMA bar while spalling of confined concrete was assumed to take place at a strain of 0.004 as suggested by Hose et al. [39]. Crushing strain of core concrete was calculated based on the equation proposed by Paulay and Priestley [28]:

$$\varepsilon_{cu} = 0.004 + 1.4\rho_s f_{yh}\varepsilon_{sm} / f_{ç} \quad (9)$$

where ε_{cu} is the ultimate compression strain, ε_{sm} is the steel strain at maximum tensile stress, f_c is the concrete compressive strength in MPa, f_{yh} is the yield strength of transverse steel in MPa, and ρ_s is the volumetric ratio of confining steel.

Table 4 shows the four limit state capacities in terms of median (Sc) and dispersion (β_c). The dispersion of limit state models was calculated using the equation developed by Nielson and Pang [27]:

$$\beta_c = \sqrt{\ln(1 + COV^2)} \quad (10)$$

A probabilistic distribution of limit states was used to calculate the coefficient of variation (COV) for each limit state and the COVs were found to be 0.21 for DS1, 0.27 for DS2, 0.41 for DS3 and 0.44 for DS4, yielding similar dispersion values Nielson and Pang [27].

The fragility curves developed for three different RC-SMA wall piers considering maximum drift as the EDP using the linear PSDMs and limit state models presented in Table 3 and Table 4 are plotted in Fig. 4. The probability of cracking damage is seen very high irrespective of the seismic intensity levels. A closer look into Fig. 4a reveals that all the wall piers possess similar level of vulnerability at the cracking damage state.

However, the effect of SMAs is more noticeable at the other damage states.

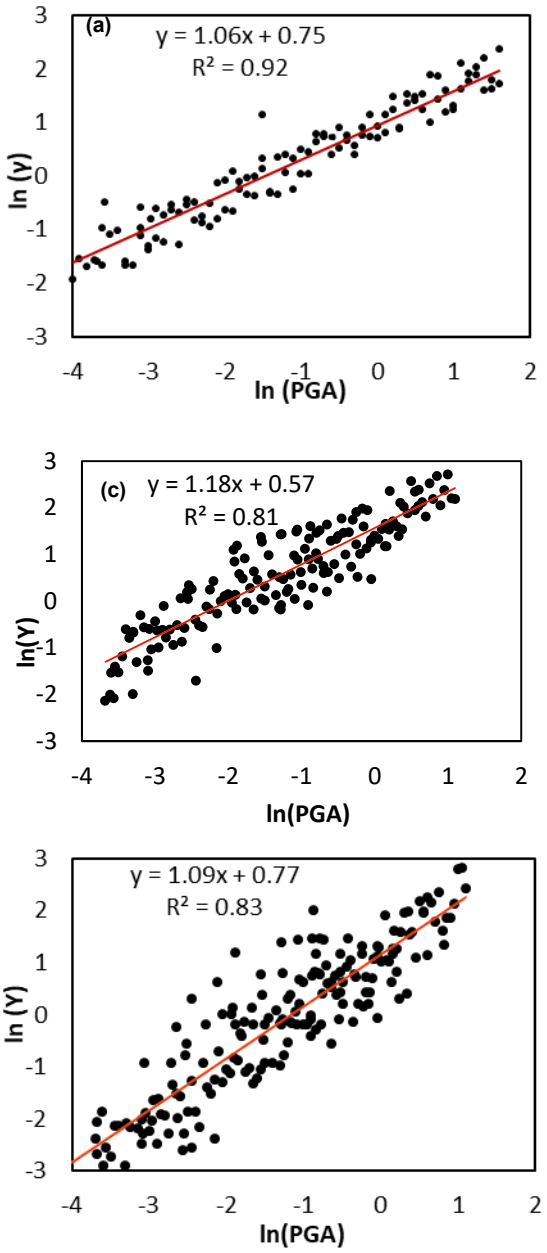

Fig. 3. Comparison of the PSDMs for (a) SMA-RC1, (b) SMA-RC2, (c) SMA-RC3, considering maximum drift as EDP

The RC-SMA1 wall pier performs better than the other two wall piers with a probability of damage of 87% if built in a seismic zone with a PGA of 2g. The high yield strength of SMA3 could have contributed to the better performance of the wall pier. It is also observed from Fig. 4c that the probabilities associated spalling for RC-SMA2 is more closed to other compare to probability of yielding damage. This can be attributed to the limit state capacity considered in this study showed that the range of spalling capacity are 1.32 – 1.35. On the other hand, the probability of crushing damage (Fig.4 d) are 20%, 35% and 18% by PGA=2g for RC-SMA1, RC-SMA2 and RC-SM3, respectively.

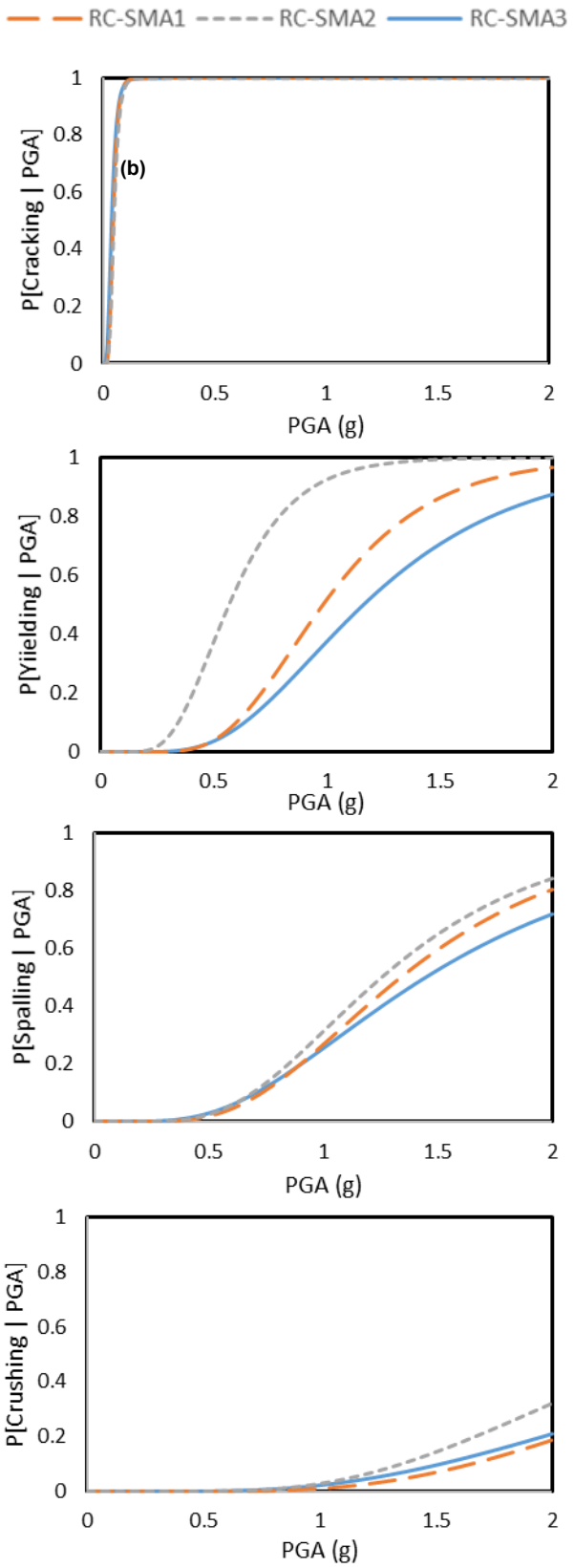

Fig. 4. Fragility curves for three RC-SMA wall pier for (a) slight, (b) moderate, (c) extensive and (d) collapse considering maximum drift as EDP

Table 5. and Fig. 4. shown the comparison of median values of PGA for different types RC-SMA wall piers in term of maximum drift. The median PGA are defined as 50% of the probability of RC-SMAs reaching a limit state. At DS1, the median PGA ranges from 0.03g up to 0.05g. This results consistent with finding from [21], which the authors found the similar ranges median values of PGA for slight damage state. When looking at higher damage state, the median PGA for RC-SMA2 was 0.58g and 1.31g for DS2 and DS3, which the lowest value than other two RC-SMAs. This results indicates that the RC-SMA2 is more fragile compare to others wall pier. On the other hand, RC-SMA1 and RC-SMA2 have almost the same median values of PGA around 3.15g and 3.19g at DS4.

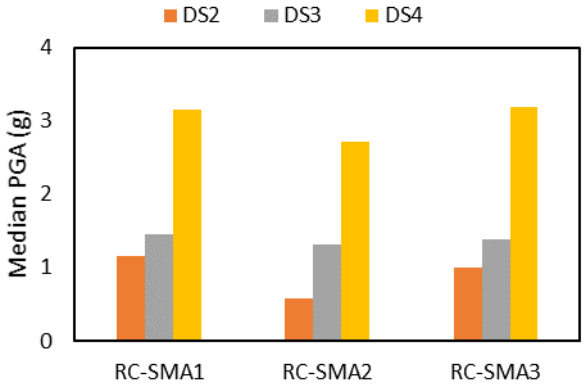

Fig. 5. Bar chart of median values of PGA for wall pier with different SMA

Table 5. Comparison of median P

EDP	Maximum Drift			
	Damage State			
Wall pier	DS1	DS2	DS3	DS4
RC-SMA1	0.05g	1.15g	1.45g	3.15g
RC-SMA2	0.03g	0.58g	1.31g	2.71g
RC-SMA3	0.03g	0.99g	1.39g	3.19g

6 Conclusion

This article presents an analytical approach to develop maximum drift fragility curves for concrete wall pier reinforced with three different of SMAs. Analytical RC-SMA wall pier models with a scaled of 20 ground motions for Seismostruct numerical software and incremental dynamic analysis are performed to generate the fragility curves. Based on the analysis results lead to the following major conclusion:

1. The mechanical properties of different shape memory alloy significantly affect the seismic vulnerability of wall pier reinforced with SMA.
2. RC-SMA2 is more vulnerable compare to other RC-SMA wall pier.
3. In general, all RC-SMA wall piers are significantly effective in reducing the vulnerability, which is exhibited low probability of collapse.
4. The RC-SMA3 are the least vulnerable of wall pier, with median PGA values for collapse damage (DS4) being 3.19g. However, the median PGA values for moderate (DS2) and extensive (DS3) damages are 0.99g and 1.39g, respectively, which more vulnerable compare to RC-SMA1.

The present study only considered maximum drift as EDP. Further study for wall pier with different geometry and material properties and also considering both the horizontal components of ground motion. Finally, the developed fragility curves provide the effect of different types of SMA on the seismic performance of wall pier. Furthermore, this RC-SMA fragility curves will help to make the effective decision making for choose of SMAs.

The work was financially supported under a postgraduate scholarship offered by the Ministry of Higher Education Malaysia (MOHE) and Universiti Teknologi MARA, Shah Alam, Malaysia (UiTM), all of whom are gratefully acknowledged.

References

1. EC8-2, (2008). Eurocode 8: Design of Structures for Earthquake Resistance—Part 2. Seismic Design of Bridges, European Committee for Standardization, Brussels, Belgium.
2. JRA 2012—Japan Road Association. Specifications for highway bridges, Part V: seismic design, Japan, 2012.
3. Canadian Standards Association. (2014). CAN/CSA-S6-14—Canadian highway bridge design code. Canadian Standards Association, Rexdale, Ontario, Canada, .894
4. American Association of State Highway and Transportation Officials (AASHTO). (2011) AASHTO Guide Specifications for LRFD Seismic Bridge Design, 2nd ed., AASHTO, Washington, D.C.
5. Billah, A.H.M., & Alam, M.S. Seismic fragility assessment of concrete bridge pier reinforced with superelastic shape memory alloy. Earthquake Spectra, 31, 1515-1541 (2015) DOI: 10.1193/112512EQS337M.
6. Rossetto, T. and Elnashai, A.S. Derivation of vulnerability functions for European type RC structures based on observational data.

Engineering Structures, 25(10):1241-1263 (2003).

7. Elnashai, A., Borzi, B., Vlachos, S. Deformation-based vulnerability functions for RC bridges, Structural Engineering and Mechanics, 17(2): 215-244 (2004).
8. Shinozuka, M., Feng, M. Q., Kim, H., Uzawa, T. Ueda, T. Statistical analysis of fragility curves, Report No. MCEER-03-0002, MCEER, University at Buffalo, The State University of New York, Buffalo, NY. (2001).
9. Vosooghi, A. and Saiidi, M.S. Experimental fragility curves for seismic response of reinforced concrete bridge columns. ACI Structural Journal, 109 (6): 825-834 (2012).
10. Banerjee, S. and Chi, C. State-dependent fragility curves of bridges based on vibration measurements, Probabilistic Engineering Mechanics, 33:116–125 (2013).
11. Alam, M.S., Bhuiyan, A.R., and Billah, A.H.M.M. Seismic fragility assessment of SMA- bar restrained multi-span continuous highway bridge isolated with laminated rubber bearing in medium to strong seismic risk zones. Bull. Earthq. Engr., 10(6): 1885- 1909 (2012).
12. Billah, A.H.M.M. and Alam, M.S. Seismic vulnerability assessment of a typical multi- span continuous concrete highway bridge in British Columbia. Accepted in Canadian Journal of Civil Engineering, Manuscript ID: CJCE-2013-0049R2. (2013).
13. Billah, A.H.M.M. and Alam, M.S. Seismic performance of concrete columns reinforced with hybrid shape memory alloy (SMA) and fiber reinforced polymer (FRP) bars. Construction and Building Materials, 28 (1): 730–742 (2012).
14. Saiidi, M.S., O'Brien, M. and Zadeh, M.S. Cyclic response of concrete bridge columns using superelastic nitinol and bendable concrete. ACI Struct J. 106(1): 69-77 (2009).
15. Roh, H., Lee, J.S. and Reinhorn, A.M. Hysteretic behavior of precast segmental bridge piers with superelastic shape memory alloy bars. Engineering Structures 32: 3394-3403 (2010).
16. Saiidi, M.S. and Wang, H. Exploratory study of seismic response of concrete columns with shape memory alloys reinforcement. ACI Struct. J. 103(3): 435-42 (2006).
17. Tazarv, M., & Saiidi, M. S. Reinforcing NiTi Superelastic SMA for Concrete Structures. Journal of Structural Engineering,141(8), 04014197. doi:10.1061/(ASCE)ST.1943-541X.0001176 (2014)
18. Billah, A.H.M.M. and Alam, M.S. (2012). Seismic performance of concrete columns reinforced with hybrid shape memory alloy (SMA) and fiber reinforced polymer (FRP) bars. Construction and Building Materials, 28 (1): 730–742.
19. Billah, A.H.M.M. and Alam, M.S. (2012b). Seismic fragility assessment of concrete bridge pier reinforced with Shape Memory Alloy considering residual displacement, in SPIE Conference on Active and Passive Smart Structures and Integrated Systems VI, 11-15 March 2012, San Diego, California, USA. 83411F:1-13.
20. Bhuiyan, A.R. and Alam, M.S. (2012). Seismic vulnerability assessment of a multi-span continuous highway bridge fitted with shape memory alloy bar and laminated rubber bearing. Earthquake Spectra, 28(4): 1379-1404.
21. Bipin Shrestha, Chao Li, Hong Hao and Hongnan Li. Performance based seismic assessment of superelastic shape memory alloy reinforced bridge piers considering residual deformations. Journal of Earthquake Engineering, 21:7, 1050-1069, DOI: 10.1080/13632469.2016.1190798 (2017).
22. Billah, A.H.M.M. and Alam, M.S. Probabilistic seismic risk assessment of concrete bridge piers reinforced with different types of shape memory alloys. Engineering Structure, 162 : 97–108 (2018).
23. Vamvatsikos, D. and Cornell, A. C. (2002). Incremental dynamic analysis. Earthquake Engineering & Structural Dynamics, 31, 491–514.
24. Billah, A.H.M.M. and Alam, M.S. Seismic fragility assessment of concrete bridge pier reinforced with Shape Memory Alloy considering residual displacement, in SPIE Conference on Active and Passive Smart Structures and Integrated Systems VI, 11-15 March 2012, San Diego, California, USA. 83411F :1-13 (2012).
25. Cornell, A.C., Jalayer, F. and Hamburger, R.O. Probabilistic basis for 2000 SAC federal emergency management agency steel moment frame guidelines. J Struct Eng, 128, 526-532 (2002).
26. Baker, J.W., Cornell, C.A. Vector-valued ground motion intensity measures for probabilistic seismic demand analysis. Pacific Earthquake Engineering Research report

2006/08, PEER Center, University of California Berkeley. (2006).

27. Nielson, B.G. and Pang, W. (2011) Effect of Ground Motion Suite Size on Uncertainty Estimation in Seismic Bridge Fragility Modeling. Structures Congress 2011: 23-34.
28. Paulay, T. and Priestley, M.N.J. Seismic design of reinforced concrete and masonry buildings. New York: John Willey & Sons, Inc. (1992).
29. SeismoSoft. SeismoStruct - A computer program for static and dynamic nonlinear analysis of framed structures (Version 6) [Software]. Available from www.seismosoft.`. (2016).
30. Mander, J. B.,Priestley, M.J.N., and Park, R. Theoretical stress-strain model for confined concrete. Journal of Structural Engineering, 114(8), 1804-1826 (1998).
31. Menegotto, M & Pinto, P.E. Method of analysis for cyclically loaded R.C. plane frames including changes in geometry and non-elastic behaviour of elements under combined normal force and bending. Symposium on the Resistance and Ultimate Deformability of Structures Acted on by Well Defined Repeated Loads. International Association for Bridge and Structural Engineering, Zurich, Switzerland, 15-22 (1973).
32. Auricchio, F., & Sacco, E. A Superelastic shape-memory-alloy beam model. Journal Intelligent Material System Structure, 8(6), 489–501 (1997).
33. Otani, S. SAKE, A Computer Program for Inelastic Response of R/C Frames to earthquakes, Report UILU-Eng-74-2029, Civil Engineering Studies, University of Illinois at Urbana Champaign. (1974).
34. Alam, M.S., Youssef, M.A., and Nehdi, M. Exploratory investigation on mechanical anchors for connecting SMA bars to steel or FRP bars, Materials and Structures 43, 91–107 (2010).
35. SeismoSoft. Seismomatch - A computer program for adjusting earthquake accelerograms to match a specific target response spectrum, using the wavelets algorithm (Version 8) [Software]. Available from www.seismosoft.com (2016).
36. Padgett, J.E., Nielson, B.G., and DesRoches, R. Selection of optimal intensity measures in probabilistic seismic demand models of highway bridge portfolios. Earthquake Engineering and Structural Dynamics, 37, 711-725 (2008).
37. Mackie, K. R., and Stojadinović, B. Performance-based seismic bridge design for damage and loss limits states, Earthquake Engineering and Structural Dynamics 36, 1953–1971. (2007).
38. Federal Emergency Management Agency (FEMA). HAZUS-MH software, Washington, D.C.(2003).
39. Hose, Y., Silva, P. and Seible, F. Development of a performance evaluation database for concrete bridge components and systems under simulated seismic loads. Earthquake Spectra; 16(2): 413-442. (2000).
40. Priestley, M.J.N., Seible, F., and Calvi, G.M. (1996). Seismic design and retrofit of bridges. Wiley, New York.